Biology of Reproduction, 2018, 99(5), 1010–1021
doi:10.1093/biolre/ioy132
Research Article
Advance Access Publication Date: 8 June 2018

Research Article

Intracellular Ca^{2+} threshold reversibly switches flagellar beat off and on†

C. Sánchez-Cárdenas[1], F. Montoya[2], F.A. Navarrete[4], A. Hernández-Cruz[3], G. Corkidi[2], P.E. Visconti[4,*] and A. Darszon[1,*]

[1]Departamento de Genética del Desarrollo y Fisiología Molecular, Instituto de Biotecnología, Universidad Nacional Autónoma de México, UNAM, Cuernavaca, Mor., México; [2]Laboratorio de Imágenes y Visión por Computadora, Departamento de Ingeniería Celular y Biocatálisis, Instituto de Biotecnología, UNAM, Cuernavaca, Mor., México; [3]Departamento de Neurociencia Cognitiva, Instituto de Fisiología Celular, UNAM, Ciudad Universitaria, México DF, México and [4]Department of Veterinary and Animal Sciences, University of Massachusetts, Amherst, Massachusetts, USA

*__Correspondence:__ Departamento de Genética del Desarrollo y Fisiología Molecular, Instituto de Biotecnología, Universidad Nacional Autónoma de México, Apdo 510–3, Cuernavaca, Morelos 62250, México. Tel: (52-555)6227650; E-mail: darszon@ibt.unam.mx
Department of Veterinary and Animal Sciences, University of Massachusetts, Amherst, Massachusetts, USA; pvisconti@vasci.umass.edu

†__Grant Support:__ This study was supported by Eunice Kennedy Shriver National Institute of Child Health and Human Development NIH (RO1 HD38082) to P.E.V. and by Consejo Nacional de Ciencia y Tecnología (CONACyT) (grants 253952 to G.C, Fronteras 71 39908-Q to A.D, and 279820 (Laboratorio Nacional de Canalopatías) and CB 240305 to AHC. The paper was also supported by the Dirección General de Asuntos del Personal Académico of the Universidad Nacional Autónoma de México (DGAPA-UNAM) (grants IN205516 to A.D, PAPIIT IN211616 to AHC and to CJIC/CTIC/4898/2016 to F. M.), by Secretaría de Ciencia, Tecnología e Innovación del Distrito Federal (SECITI).
Edited by Dr. Jeremy P. Wang, MD, PhD, University of Pennsylvania.

Received 17 October 2017; Revised 9 March 2018; Accepted 7 June 2018

ABSTRACT

Sperm motility is essential for fertilization. The asymmetry of flagellar beat in spermatozoa is finely regulated by intracellular calcium concentration ($[Ca^{2+}]_i$). Recently, we demonstrated that the application of high concentrations (10–20 μM) of the Ca^{2+} ionophore A23187 promotes sperm immobilization after 10 min, and its removal thereafter allows motility recovery, hyperactivation, and fertilization. In addition, the same ionophore treatment overcomes infertility observed in sperm from Catsper1$^{-/-}$, Slo3$^{-/-}$, and Adcy10$^{-/-}$, but not PMCA4$^{-/-}$, which strongly suggest that regulation of $[Ca^{2+}]_i$ is mandatory for sperm motility and hyperactivation. In this study, we found that prior to inducing sperm immobilization, high A23187 concentrations (10 μM) increase flagellar beat. While 5–10 μM A23187 substantially elevates $[Ca^{2+}]_i$ and rapidly immobilizes sperm in a few minutes, smaller concentrations (0.5 and 1 μM) provoke smaller $[Ca^{2+}]_i$ increases and sperm hyperactivation, confirming that $[Ca^{2+}]_i$ increases act as a motility switch. Until now, the $[Ca^{2+}]_i$ thresholds that switch motility on and off were not fully understood. To study the relationship between $[Ca^{2+}]_i$ and flagellar beating, we developed an automatic tool that allows the simultaneous measurement of these two parameters. Individual spermatozoa were treated with A23187, which is then washed to evaluate $[Ca^{2+}]_i$ and flagellar beat recovery using the implemented method. We observe that $[Ca^{2+}]_i$ must decrease below a threshold concentration range to facilitate subsequent flagellar beat recovery and sperm motility.

Summary Sentence

A novel semiautomatized tool that simultaneously monitor [Ca^{2+}]$_i$ and motility reveals the requirement of a [Ca^{2+}]$_i$ threshold for flagellar beating control.

Key words: sperm, sperm motility, calcium.

Introduction

Spermatozoa acquire fertilizing capacity in the female tract in a process known as capacitation. As part of capacitation, sperm change their motility pattern (i.e., hyperactivation) and acquire the ability to undergo a physiologically induced acrosome reaction. At the molecular level, capacitation is associated with a fast increase in cAMP synthesis followed by activation of the cAMP-dependent kinase (PKA). In addition, capacitation induces changes in the concentration of intracellular calcium ([Ca^{2+}]$_i$). Pharmacological and genetic loss-of-function experiments have shown that both cAMP and Ca^{2+}-dependent pathways are involved in capacitation (for review see [1]). In particular, it has been shown that cAMP increases the frequency of flagellar beating and that Ca^{2+} is required for the increased asymmetry of flagellar movement associated with hyperactivation (reviewed in [2, 3]). On the other hand, Ca^{2+} gain-of-function experiments showed that addition of Ca^{2+} ionophore A23187 produced a fast increase in [Ca^{2+}]$_i$ accompanied by complete loss of sperm motility [4, 5]. However, after washing out the Ca^{2+} ionophore, sperm gained hyperactive motility and fertilizing capacity even when PKA was inhibited. These experiments suggested that a transient exposure to A23187 could be used to overcome defects in capacitation-associated signaling. Indeed, we recently showed that the short A23187 incubation approach induced hyperactivation and fertilization capacity in vitro of spermatozoa from sterile mice models, such as those lacking the sperm-specific Ca^{2+} channel complex CatSper (CatSper1$^{-/-}$), the sperm-specific K^+ channel SLO3 (Slo3$^{-/-}$), and the atypical soluble adenylyl cyclase Adcy10 (Adcy10$^{-/-}$) [6].

Altogether, these data suggest that the effect of intracellular Ca^{2+} concentration ([Ca^{2+}]$_i$) on sperm motility is biphasic. On the one hand, an increase in [Ca^{2+}]$_i$ is required for hyperactivation; however, when it becomes too high after exposure to A23187, sperm stop moving. At present, it is not known why flagellar movement is inhibited in these conditions; however, the aforementioned experiments clearly showed that this A23187 effect is reversible, suggesting that upon washing the A23187 ionophore, [Ca^{2+}]$_i$ is reduced to a threshold concentration that removes the block.

Sperm flagellar regulation depends on the coordinated interplay of external and internal parameters and the molecular events occurring in the flagellum. Among them, [Ca^{2+}]$_i$ plays a central role. Given the large number of linear and nonlinear variables that arise from Ca^{2+} interactions, theoretical models are needed to gain a better insight into the essential features of the system (reviewed by [2, 7]). In addition to the usefulness of models as descriptive tools, they provide predictive frameworks for hypothesis generation and the possibility of addressing questions that are experimentally unanswerable at present due to technical limitations. A model for hyperactivation in mammalian spermatozoa was developed considering some detailed signaling processes pertaining to flagellar beating and its ensuing hydrodynamic implications [8]. However, signaling, detailed [Ca^{2+}]$_i$ changes and motor responses have not been integrated yet.

In this work, we examined if there are different thresholds for motility inhibition and activation by determining sperm motility under different A23187 treatments, alongside simultaneously measuring [Ca^{2+}]$_i$ and flagellar beating in sperm attached to laminin-coated coverslips. Throughout the text we use the term flagellar beating when qualitatively determining flagella movement in relation to its initiation or inhibition, or more precisely, as a change in the midpiece curvature over time. The extent to which flagellar beating depends on a [Ca^{2+}]$_i$ threshold was investigated using imaging techniques designed to mathematically correlate [Ca^{2+}]$_i$ with flagellar beating. To achieve this, we defined a flagellar angle by considering how the sperm flagellar midpiece oscillates in relation to a fixed point in the head and plotted changes in the variance (S^2) of this flagellar angle as a function of time. We found that (1) [Ca^{2+}]$_i$ can be controlled by limiting A23187 concentrations and that the ionophore effect is time dependent; (2) A23187 removal resulted in [Ca^{2+}]$_i$ reduction which was correlated with an increase in flagellar movement; and (3) the use of the S^2 function indicates that after removing A23187, movement is re-initiated only when [Ca^{2+}]$_i$ falls below a threshold concentration.

Materials and methods

Sperm preparation

Experimental protocols were approved by the University of Massachusetts and the Instituto de Biotecnología/UNAM Animal Care Committees. In all experiments, cauda epididymal mouse sperm were collected from CD1 mature males (10–12 weeks old) by swim-up in Toyoda–Yokoyama–Hosi (TYH) media at 37°C for 15 min. TYH medium contains 119.4 mM NaCl, 4.7 mM KCl, 1.7 mM $CaCl_2.2H_2O$, 1.2 mM KH_2PO_4, 1.2 mM $MgSO_4.7H_2O$, 0.5 mM Na-pyruvate, 5.6 mM glucose, 20 mM HEPES, and 5 mg/ml bovine serum albumin (BSA) only to wash. The medium was maintained at pH 7.3.

Live [Ca^{2+}]$_i$ imaging in individual mice sperm

For [Ca^{2+}]$_i$ recordings, the obtained sperm were incubated with 2 μM Fluo-4 AM and 0.05% Pluronic acid during 40 min in TYH under noncapacitating conditions. Once loaded, sperm were immobilized on mouse laminin (1 mg/ml) coated cover slips. Unattached spermatozoa were removed by gentle washing and the chamber was filled with recording medium (TYH). Recordings were performed at 37°C using a temperature controller (Harvard Apparatus, model 202A). Sperm were viewed with an inverted microscope (Nikon Eclipse Ti-U) and an oil immersion fluorescence objective (Nikon plan Apo TIRF DIC H/N2 60x/1.45 NA). A pre-centered fiber illuminator, Nikon Intensilight-CHGFI (Nikon), was used as the light source. For excitation and emission collection of Fluo-4 fluorescence, the filter set GFP 96343, D: 495, Exc: 470/40, barrier 525/50 (Nikon) was used. Fluorescence images were acquired with an Andor Ixon 3 EMCCD camera model DU-8970-C00#B (Andor Technology) under protocols written in Andor iQ 1.10.2 software version 4.0. Imaging experiments were recorded at different frequencies depending on the particular requirements of each protocol. Slow capture protocols were performed at 1 or 0.2 frames per second (FPS), while fast capture protocols were performed at 40–50 FPS.

A23187 incubation and washing protocol

For A23187 incubation, Fluo-4 loaded noncapacitated sperm were attached to laminin-treated coverslips at low concentrations (density) to allow appropriate semiautomated detection. In these experiments, sperm were incubated with 10 μM A23187 during 10 min until immobilized. For control experiments, 10 μM A23187 was maintained without washing. The A23187 washing protocol consisted of completely removing the solution and refilling the recording chamber with A23187-free TYH BSA supplemented media three times before starting the recordings. Randomly selected single spermatozoon were recorded for 2–7 min until finding one which started moving.

Sperm motility analysis using CASA

Mice cauda sperm were collected from CD-1 males described above. Both cauda epididymis were placed in 1 ml of TYH media. After 10 min, incubation at 37°C (swim-out), epididymal tissue debris were removed, and the suspension adjusted to a final concentration of 1–2 $\times$ 10^7 cells/ml and divided into five aliquots with 15 mM HCO^-_3 and 15 mg/ml BSA. Four aliquots were supplemented with 0.5, 1, 5, and 10 μM A23187 and to the final aliquot an equivalent final concentration of DMSO (as a control) and further incubated at 37°C. Afterwards, sperm cell hyperactivation and motility percentage were measured at time points 1, 2, 3, 10, and 60 min by CASA system (Hamilton Thorne Research, Beverly, MA). The default settings include the following: frames acquired: 90; frame rate: 60 Hz; minimum cell size: 4 pixels; static head size: 0.13–2.43; static head intensity: 0.10–1.52; static head elongation: 5–100. Sperm with hyper activated motility, defined as motility with high amplitude thrashing patterns and short distance of travel, were sorted using the criteria established by Goodson et al. [9]. The data were analyzed using the CASA nova software [9]. At least 20 microscopy fields corresponding to a minimum of 200 sperm were analyzed in each experiment.

Semiautomatized detection program implementation

Fluorescence TIFF image stacks were processed using an FFT (Fast Fourier Transform) spatial bandpass filter embedded in the ImageJ software (https://imagej.nih.gov/ij/). The criterion to define the parameters of the filter depends on the experimental setup. In our case, the goal was to enhance the structures between 3 and 40 pixels of width, where the lower limit corresponds to the flagellar width and the upper limit to the head size. After the filter, a threshold binarization splits the image into information corresponding to the cell and the background. A homemade algorithm written in java with the Netbeans IDE software 8.1 (https://netbeans.org/index.html) was implemented to split the cell into two main regions, the flagellum midpiece and the head (Figure 5, center panel). The implemented algorithm was able to simultaneously measure fluorescence, area of the midpiece, and angle changes between head (independently) and midpiece. The "center of mass" of the head was estimated through the coordinates obtained from the segmentation information (blue area). This point is shown as P1 in Figure 5E and F. Assuming a constant density, the center of mass was estimated as:

$$\overrightarrow{r_{cm}} = \frac{1}{m} \sum \overrightarrow{r_i}$$

where the set$\{r_i\}_{i=1}^{m}$ corresponds to the coordinates of the pixels that integrate the area of the head. Figure 5E shows, at the beginning and the end of the midpiece, points P2 and P3, respectively. These points were found through the connected components algorithm. As shown in Figure 5E, right panel, the P1 and P2 points define a vector that goes from the center of the head to the beginning of the middle piece; P1 and P3 define a vector that begins in the center of the head and finishes at the end of the midpiece. The angle between these two vectors was calculated as $angle = arcsin(\frac{|AxB|}{|A||B|})$, and is an estimate of the curvature of the midpiece. We refer to this angle as γ since it is equivalent, but not the same, to the α angle measured by [10]. To more clearly detect when and how the flagellum is beating over time, the instantaneous variance (S^2) of the angle γ, defined as its variance estimated within a small temporal window, as compared to the total length of the original time series. Its mathematical definition is as follows:

$$S^2\ (t) = \frac{1}{\Delta t} \sum_{(i=t)}^{(t+\Delta t)} \left(\theta\ (i) - \theta_{(mean,\Delta t)}\right)^2,$$

where θ is the original variable that measures the curvature of the flagellum, Δt is the temporal window size over the summation, $\theta_{(mean,\ \Delta t)}$ is the average in the interval (t, t + Δt), and σ(t) is the instantaneous variance as a function of the time, which takes values in the interval 1 $\leq$ t $\leq$ N-Δt, where N is the total length of the time series. In the context of this work, Δt = 50, N$\sim$5000. Small values of $S^2(t)$ represent a nearly immotile flagellum, while large values indicate vigorous movement. Significant changes in S^2 reflect transitions from immotility to dynamic activity of the flagellum, or vice versa. This representation of flagellar movement was chosen instead of the angle because it eliminates a significant amount of noise that comes from the segmentation process. Figure 5F shows an example of these two variables.

Statistical analysis

Results were statistically analyzed using a Student *t*-test employing Origin software 6.0.

Results

We have previously shown that spermatozoa become immotile after incubation with Ca^{2+} ionophore A23187 for 10 min; however, when the ionophore is washed out by centrifugation, motility recovers and sperm undergo hyperactivation. These data suggest that there is a direct relationship between $[Ca^{2+}]_i$ and sperm motility. To evaluate this possibility, we added 10 μM A23187 to Fluo-4-loaded mice spermatozoa and simultaneously recorded $[Ca^{2+}]_i$ changes and flagellar beating in sperm attached to laminin. These sperm are bound to the slide by their head; in spite of this, their flagella are freely moving and can be observed via time lapse recording. Figure 1A, upper panel, and Supplemental Movie 1 show that A23187 addition promotes a rapid and sustained $[Ca^{2+}]_i$ increase in all sperm in the field, as indicated in the example shown in the right panel trace. These images also revealed that after 10 min most sperm become completely immotile as previously reported. However, at shorter time points (5–20 s) after A23187 application, this ionophore transiently induces vigorous motility. This phenomena can be clearly observed in Figure 1B that illustrates two sperm from Figure 1A (see white rectangle at the image corresponding to 100 s in Figure 1A and Supplemental Movie 2) viewed at higher magnification. Blue and yellow arrows in these images indicate the positions of sperm tails which show considerable changes in flagellar movement observed shortly after A23187 addition and the image sequence shows that these changes in flagellar beating were accompanied by fluorescence increases in the indicated sperm. These images were obtained at relatively low time resolution (0.45 FPS) which makes it difficult to observe the beating of the sperm flagella. Therefore, to observe flagellar beating,

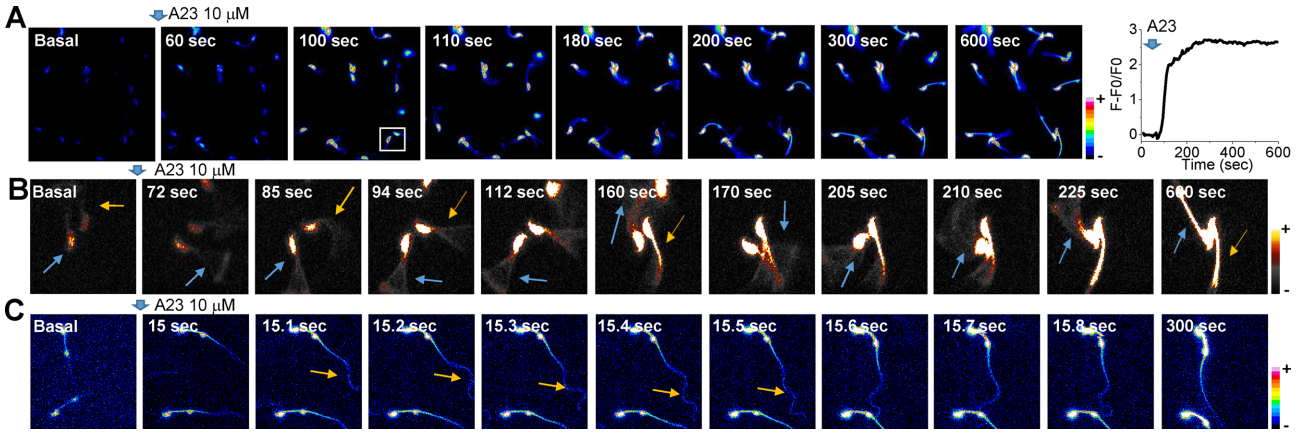

Figure 1. [Ca^{2+}]$_i$ response promoted by 10 μM A23187 increases flagellar beating before producing sperm immobility. (A) Time series of fluorescence images showing that 10 μM A23187 application promotes a rapid and sustained [Ca^{2+}]$_i$ increase in mouse spermatozoa. The sustained [Ca^{2+}]$_i$ increase leads to immobility of all spermatozoa in the field towards the end of the recording (see panels at 300–600 s). (B) Fluo-4 fluorescence still images at different times correspond to a zoom area of Figure 1A (see white rectangle) illustrating that A23187 application increases flagellar beat (indicated by blue and yellow arrows) before producing sperm immobility at longer times. (C) Fluorescence images obtained at 10/FPS showing that A23187 application increases principal piece beating that stops at sec 300 (n = 4 mice). (Please see the online version for the color figure.)

the same experiments were conducted at a greater time resolution (8–10 FPS). While conducting these experiments, we observed that, before becoming immobilized, most spermatozoa showed a temporary increase in the sperm flagellar beating shortly after addition of A23187; this phenomena can be clearly observed in Supplemental Movie 3 and Figure 1C (yellow arrow). These findings suggest that the relationship between [Ca^{2+}]$_i$ and flagellar beating is biphasic. While [Ca^{2+}]$_i$ elevation increases flagellar beating, once a threshold concentration is surpassed, Ca^{2+} activates signaling pathways that negatively regulate sperm movement.

To further test the relationship between [Ca^{2+}]$_i$ and motility, sperm loaded with Fluo-4 were incubated in the presence of increasing A23187 concentrations (0.5, 1, 5, and 10 μM), attached to laminin, and fluorescence and flagellar movement monitored simultaneously (Figure 2). The fluorescence time projections in Figure 2A and the corresponding [Ca^{2+}]$_i$ traces in Figure 2B show representative results of these experiments. Images and traces illustrate that the kinetics and magnitude of the [Ca^{2+}]$_i$ changes depend on the A23187 concentration applied. To evaluate how different [Ca^{2+}]$_i$ levels correlated with flagellar beating, temporally integrated images created using Image J (https://imagej.nih.gov/ij/) are shown in Figure 2A. These temporal projections represent the maximum intensity value obtained for each pixel in the Ca^{2+} image stacks, over a 30-s sampling window applied in basal conditions, and again at both 2- and 10-min post-application of A23187 (Figure 2C). Because these images combine many frames, in motile flagella the increase in [Ca^{2+}]$_i$ is spatially integrated across neighboring pixels (i.e., 2 min, 5 μM A23187). In contrast, static flagella (10 μM A23187) remain confined to a smaller pixel array and integrate the Ca^{2+} increase across a wide group of pixels. In the case of 0.5 μM A23187, the spatial distribution of the Ca^{2+} signal is broad, but because [Ca^{2+}]$_i$ is lower, there is less fluorescence. Overall, the temporal projection allows qualitative monitoring of flagellar beating changes within a 30-s time window. These results demonstrate that higher [Ca^{2+}]$_i$ levels are reached at earlier times when higher A23187 concentrations are applied. Consistent with an inhibitory Ca^{2+} effect at high concentrations, flagellar beating was inversely correlated to A23187 concentration. Interestingly, in the presence of 0.5 and 1 μM A23187, spermatozoa remained motile after a 10-min exposure. We further quantified the percentage of immobilized spermatozoa at varying times following treatment with different A23187 concentrations. Bars in Figure 2C indicate that [Ca^{2+}]$_i$ changes and motility are related. While higher A23187 concentrations (5 and 10 μM) promote flagellar immobilization, lower concentrations (1 and 0.5 μM) do not.

Although single-cell experiments shown in Figures 1 and 2 were indicative of a biphasic [Ca^{2+}]$_i$ effect upon flagellar beating, in these experiments, spermatozoa were attached to coverslips. To analyze the extent to which [Ca^{2+}]$_i$ increases affect swimming parameters in entirely free-swimming spermatozoa, we evaluated their flagellar movement using computer assisted sperm analysis performed with the CASAnova software [9] (Figure 3 and Supplemental Figure S1). Consistent with our observations with laminin-attached sperm, all A23187 concentrations initially increased the overall percentage of progressive (Supplemental Figure S1) and hyperactive sperm (Figure 3B–E) when compared with controls obtained using standard capacitation media (Figure 3A). However, while the lowest concentration tested (0.5 μM) maintained and increased the percentage of hyperactive cells even after 60 min of incubation, higher A23187 concentrations stopped sperm movement and consequently hyperactivation in less than 10 min (Figure 3 and Supplemental Figure S1). Altogether, these results suggest that there are two [Ca^{2+}]$_i$ thresholds involved in sperm motility regulation; the first associated with the initiation of hyperactivation and a higher threshold that results in a complete cessation of motility. An alternative experimental design to examine the [Ca^{2+}]$_i$ threshold would be to rapidly increase [Ca^{2+}]$_i$ through treatment with 10 μM A23187 and then let the [Ca^{2+}]$_i$ decrease by washing out the ionophore [5]. Population analyses indicate that under these experimental conditions, motility and hyperactivation are rescued (Figure 3F; [5]). Therefore, to test the hypothesis that a particular [Ca^{2+}]$_i$ threshold is associated with the rescue of motility, [Ca^{2+}]$_i$ and flagellar beating were analyzed simultaneously in single sperm. Briefly, sperm were loaded with Fluo-4 for 30 min in noncapacitating medium supplemented with BSA and then attached to laminin-coated coverslips. Once attached, the cells were exposed to 10 μM A23187 either continuously throughout the

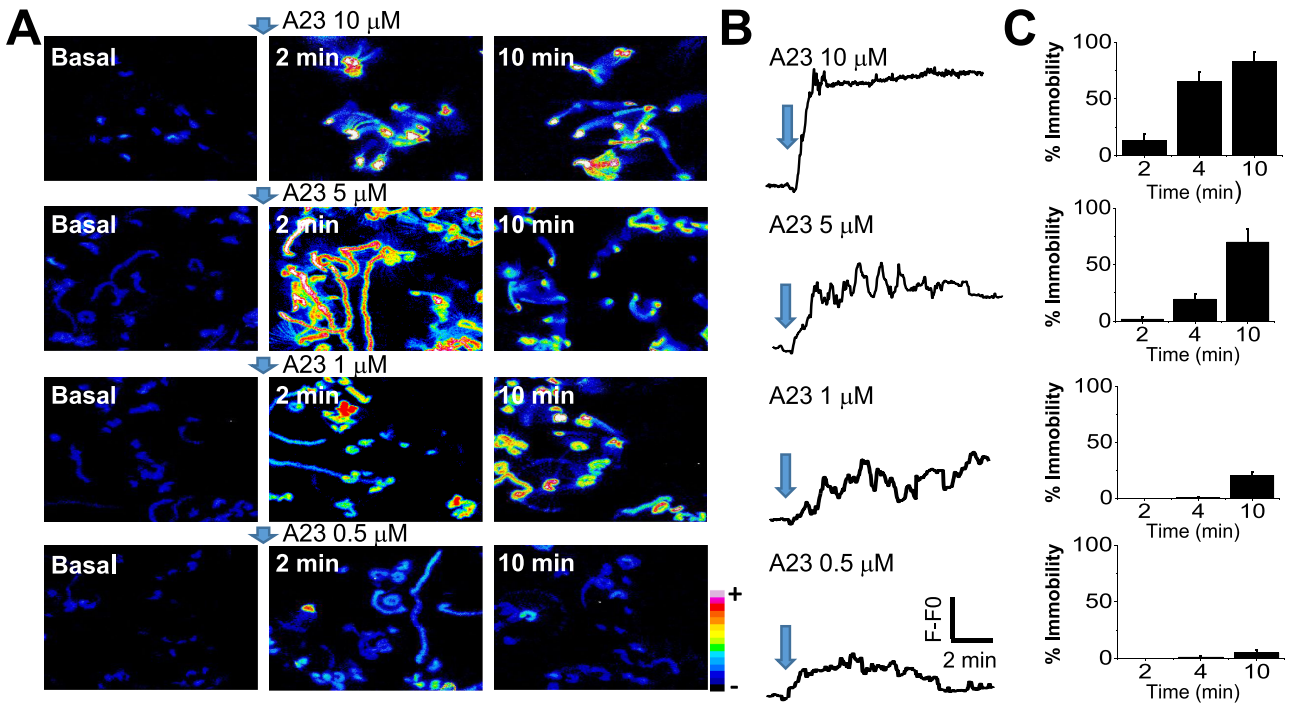

Figure 2. $[Ca^{2+}]_i$ levels and sperm motility regulation depend on the concentration of A23187 applied. (A) Time projection analysis integrating 30 s of the $[Ca^{2+}]_i$ image stacks recorded at basal condition, after 2 and 10 min of the A23187 addition. (B) Representative traces corresponding to $[Ca^{2+}]_i$ responses of spermatozoa exposed to different A23187 concentrations. (C) Bar quantification of percentage of sperm immobility observed at 2, 4, and 10 minutes after each A23187 concentration applied (average ± SEM; n = 4 mice). (Please see the online version for the color figure.)

experiment, or after 10-min incubation the A23187 was washed out. Sperm were observed for 30 min at a rate of 12 frames per minute. Fluorescence images in Figure 4 indicate that sperm in continuous presence of A23187 maintained saturating Fluo-4 fluorescence levels during the whole period (Figure 4A and A' and Supplemental Movie 4). In addition, motility quantification indicates that sperm become immotile in less than 10 min (Figure 4A" and Supplemental Movie 4). On the other hand, when A23187 was removed after 10 min of incubation, $[Ca^{2+}]_i$ decreased (Figure 4B and B') and flagellar beating recovered (Figure 4B" and Supplemental Movie 5). Notably, each spermatozoon showed different kinetics of fluorescence decrease and motility recovery (see the accumulative summary in Figure 4B"). These results are consistent with previous evidence from our group indicating that when high A23187 concentrations are washed-out, sperm motility recovers and cells undergo hyperactivation [5].

To enhance our ability to simultaneously detect $[Ca^{2+}]_i$ and motility, it is necessary to evaluate Fluo-4 fluorescence and movement of single sperm at a higher time resolution (e.g., 40 FPS), which required decreasing fluorescence light exposure to avoid cell damage. For these experiments, Fluo-4 loaded sperm were attached to laminin and exposed for 10 min to A23187 (10 μM). After this period, the treatment was either continued (Figure 5A) or ionophore was removed (Figure 5B), and changes in fluorescence and movement of single spermatozoa monitored for periods ranging from 1 to 3 min depending on the dynamic recovery of each cell. Examples of single A23187-treated spermatozoa under these conditions are illustrated in this figure. To determine $[Ca^{2+}]_i$ levels of single sperm at the moment when they recover motility, a semi-automatized image analysis protocol was designed and implemented for the data presented in Figure 5A and B, as described in Methods. Fluorescence image temporal stacks (Figure 5C, left panel) were filtered using a spatial bandpass filter and a binary threshold was applied. Once processed, we applied the sequence of algorithms described in the Methods section to segment the sperm midpiece and head regions (Figure 5C, right panel). Using this strategy, we measured fluorescence changes corresponding to $[Ca^{2+}]_i$ variations in the sperm head as a function of time (Figure 5D and D'). The head was chosen as it remained in the focal imaging plane at all times. An example of the automated determination of $[Ca^{2+}]_i$ changes is plotted in Figure 5D".

Complementary to fluorescence which is measured in a given image area, to estimate flagellar beating, it is necessary to follow changes in the position of the flagellum as a function of time. For this purpose, we defined three detection points, as follows: one in the center of the head (Figure 5E, P1), the second point in the midpiece immediately below the junction with the head (Figure 5E, P2), and the last point in the final section of the midpiece (Figure 5E, P3). To formulate a quantitative parameter, we define two vectors, one from P1 to P2 (A in Figure 5E) and the other one from P1 to P3 (B in Figure 5E). The angle γ between these two vectors is a measure of the curvature of the midpiece (Figure 5E and material and methods for detailed information). The angular variation of midpiece curvature as a function of time was automatically detected in the spermatozoon shown in Figure 5F and plotted in Figure 5F'. When the spermatozoon is not moving, the angle remains almost constant (except for noise inherent to the measurement); on the other hand, once movement begins the curvature angle varies continuously. A convenient way to represent the alterations in γ angle over time (S^2)

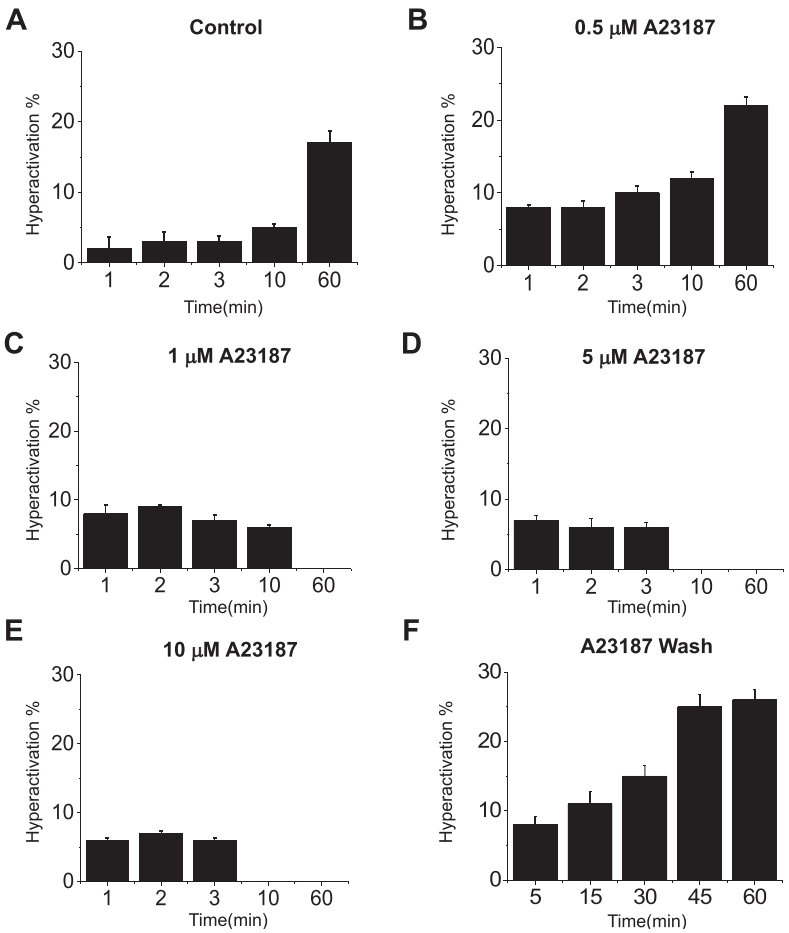

Figure 3. Hyperactivation at different A23187 concentrations measured by CASA. Sperm treated with different A23187 concentrations (0.5, 1, 5, 10 μM) were monitored at different time points 1, 2, 3, 10, 60 minutes to evaluate hyperactivation. (A) Control spermatozoa (without A23187) during capacitation. Spermatozoa treated with A23187 at: (B) 0.5 μM, (C) 1 μM, (D) 5 μM, and (E) 10 μM. (F) Spermatozoa treated with 20 μM of A23187 for 10 min and then washed by centrifugation. Hyperactivation was measured at different time points 5, 15, 30, 45, and 60 min. Bars represent average ± SEM. The percentage of hyperactive motile spermatozoa was obtained using CASAnova software (n = 3).

is by measuring and representing its variance over a rolling window of 50 time points. This parameter improves the signal-to-noise ratio in determining the angular variation of curvature over time and identification of the time at which motility is rescued (see Figure 5F").

Considering that angle evaluations are based on the continuous detection of points P1, P2, and P3, and taking into account that the image analysis procedure is semiautomated, the algorithm was programmed to discard data from spermatozoa whose flagella exit the focal plane during the course of the experiment. Out-of-focus events were detected using a pixel map of the sperm surface (Supplemental Figure S2A) and measuring the number of pixels in each segmented region over time. An example of a sperm midpiece exiting the focal plane during recording is shown in panels corresponding to 28 and 43 s (Supplemental Figure S2B). The algorithm recognizes that the analyzed region remained in focus when the pixel area value remains constant; when this variable drops to zero, the program considers that the corresponding region is completely out of focus (Supplemental Figure S2C). Cells identified as being out of focus were eliminated from the analyses. We evaluated the [Ca^{2+}]$_i$ and the variance of flagellar midpiece curvature in spermatozoa obtained from several mice (n = 10). The results obtained from spermatozoa exposed to 10 μM A23187 without washing are illustrated in Figure 6A, while those recorded from spermatozoa incubated with 10 μM A23187 and thereafter washed are shown in Figure 6B. Upper panels in Figure 6A and B display single representative sperm fluorescence images obtained during the experiments. Lower panels in the same figures illustrate the same sequence after semiautomated segmentation and filtering. Graphs on the right display [Ca^{2+}]$_i$ and the S^2 of the midpiece curvature angle changes observed during the experiments as a function of time. The results obtained from these analysis indicate that in the continued presence of A23187 both [Ca^{2+}]$_i$ and S^2 of angle γ remain unchanged, while after A23187 washing a [Ca^{2+}]$_i$ decrease is clearly observed, followed by an increase in S^2 angle when spermatozoa start to move.

To evaluate the [Ca^{2+}]$_i$ changes observed when immobilized spermatozoa recover their flagellar beat after A23187 washing, we quantified and compared the results obtained under two types of experimental protocols: in the first, spermatozoa were exposed to A23187 which was maintained for the extent of the recording, preventing motility; in the second, spermatozoa were incubated with A23187, but the ionophore was washed away before starting the experiment. Figure 7A illustrates, with different colors, individual sperm [Ca^{2+}]$_i$ recordings normalized as F-F0/F0 in both unwashed A23187 (left panel) and washed conditions (right panel). In the case

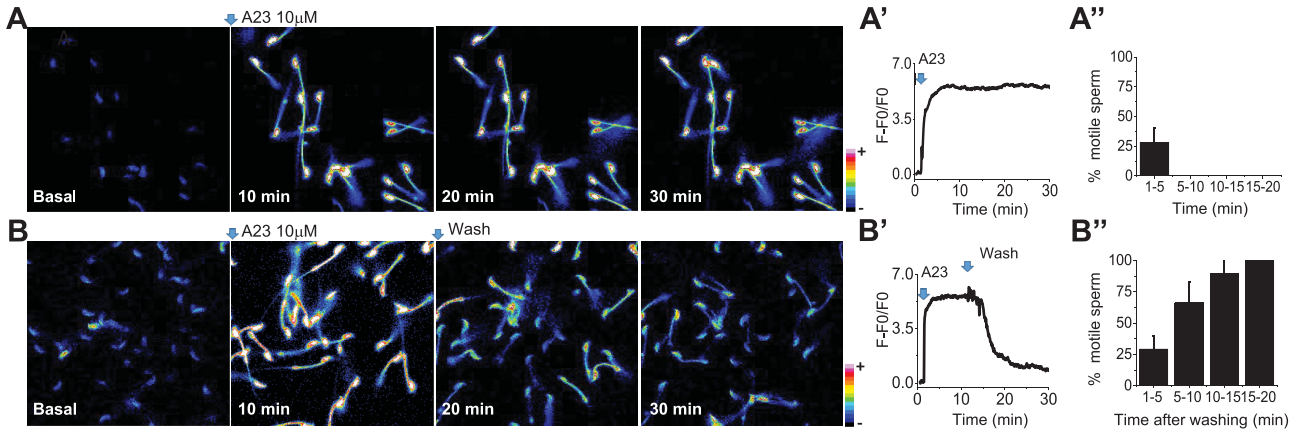

Figure 4. Removal of 10 μM A23187 restores $[Ca^{2+}]_i$ levels and motility. (A) Fluorescence time images show that a 10 μM A23187 addition maintains $[Ca^{2+}]_i$ elevated and sperm immobility even after a 30-min recording. A'. The fluorescence trace illustrates $[Ca^{2+}]_i$ levels observed in the field during the recording. (A'') Percentage of motile spermatozoa observed at different times after A23187 application. (B) Fluorescence images illustrate that after 10 min of incubation A23187 removal promotes a $[Ca^{2+}]_i$ decrease to levels similar to basal conditions (B'). (B'') A $[Ca^{2+}]_i$ decrease is followed by sperm flagellar beat recovery observed at 15 and 20 min after A23187 washing. (Please see the online version for the color figure.)

of the washed condition, the traces illustrate $[Ca^{2+}]_i$ changes corresponding to spermatozoa that recovered flagellar movement. When A23187 is not washed, $[Ca^{2+}]_i$ levels remain elevated and stable, and fluorescence photobleaching is not significant during this time interval. In contrast, individual recordings on the right panels of Figure 7A show that previous removal of A23187 induces a continuous $[Ca^{2+}]_i$ decrease in those sperm that recover flagellar beating. Figure 7B, left panel, summarizes results obtained in Figure 7A by subtracting the fluorescence at the end of the experiment (FF) observed in individual sperm after 2–3 min of recording minus the fluorescence after A23187 treatment (F0). More negative values (~–0.025) correspond to larger changes in $[Ca^{2+}]_i$ of A23187 washed sperm that recovered motility, while values close to zero (~–0.003) correspond to minimal changes in $[Ca^{2+}]_i$ levels in cells that were not washed. The difference between these two conditions is statistically significant ($P < 0.001$). This observation was confirmed by the slope analysis of the normalized traces (F-F0/F0) during the $[Ca^{2+}]_i$ determinations presented in Figure 7A. The results are shown on the right panel of Figure 7B, which indicates that more negative slopes are observed in cells after A23187 washing. We show that flagellar beat recovery requires that $[Ca^{2+}]_i$ levels decrease before sperm initiate flagellar movement following conditions of high intracellular Ca^{2+} levels induced by Ca^{2+}-ionophore treatment.

Next, we examined the extent to which a $[Ca^{2+}]_i$ threshold corresponds to the time at which the flagella regain their beating. For this purpose, we analyzed washed spermatozoa comparing the $[Ca^{2+}]_i$ of those that recovered motility vs. those that did not. To evaluate the $[Ca^{2+}]_i$ (defined as normalized fluorescence intensity) and its relationship to the recovery of flagellar beating, we aligned in time the $[Ca^{2+}]_i$ and S^2 (semi-automated measure of variance of flagellar midpiece curvature) traces; examples of these traces are illustrated in Figure 7C. For further examination, we determined a fluorescence value for each spermatozoon, classifying if they had recovered or not their flagellum motility. The blue arrows in Figure 7C indicate the time at which $[Ca^{2+}]_i$ and S^2 were measured and plotted in D. In washed spermatozoa that failed to recover motility, the time considered was at the end of the recording, as a measurement of photobleaching, whereas for the case of spermatozoa that recovered their motility after being treated with A23187, then washed, we recorded the relative decrease in Ca^{2+} level when S^2 changed. In Figure 7D (left panel), we calculated the Δ value obtained from subtracting the initial fluorescence value observed at the beginning of the recording (IF) minus the value of fluorescence observed when the S^2 change was detected (when S^2 increases above 3 standard deviations) for the recovery condition, and at the end of the experiment for the nonrecovery condition. The bars in Figure 7D, left panel, show that larger differences are observed in sperm that recover flagellar beating after washing out of A23187. The difference between conditions is statistically significant with a $P = 0.016$. Finally, Figure 7D, right panel, shows a histogram of the number of sperm displaying a certain percentage of fluorescence, considering the maximal fluorescence induced by A23187 as 100%, when their flagella started moving. The results illustrate that flagellar beating initiates when sperm attain a relatively narrow range of percent fluorescence values, i.e., $[Ca^{2+}]_i$ levels, that is consistent with the existence of a threshold. Overall, these findings indicate that after being paralyzed by a large $[Ca^{2+}]_i$ increase due to A23187 addition, removal of the ionophore allows $[Ca^{2+}]_i$ to decrease, and upon reaching a threshold, the mouse sperm flagella starts to beat.

Discussion

Ca^{2+} is one of the key signaling molecules in sperm function. This ion is essential for the spermatozoa to undergo hyperactivation and acrosomal exocytosis. Though the regulation of flagellar beating is indeed fundamental for reaching the egg and accomplishing fertilization, we are far from fully understanding molecularly how Ca^{2+} is involved. In the mammalian sperm flagellum, Ca^{2+} influx is controlled mainly by CatSper [11], a sperm-specific Ca^{2+} channel formed by multiple subunits [12–16]. Recently, CatSper was shown to localize to a newly described structure composed of four longitudinal domains present in the flagellar principal piece [17]. In addition to CatSper, these unique longitudinal structures are also sites for association of other Ca^{2+}-dependent signaling proteins, calmodulin kinase II (CaMKII), and PPP3CC (aka PP2B-Aγ and calcineurin). Altogether, these proteins appear to form signal transduction complexes mediating Ca^{2+} effects on sperm motility [17]. However, how Ca^{2+} regulates each

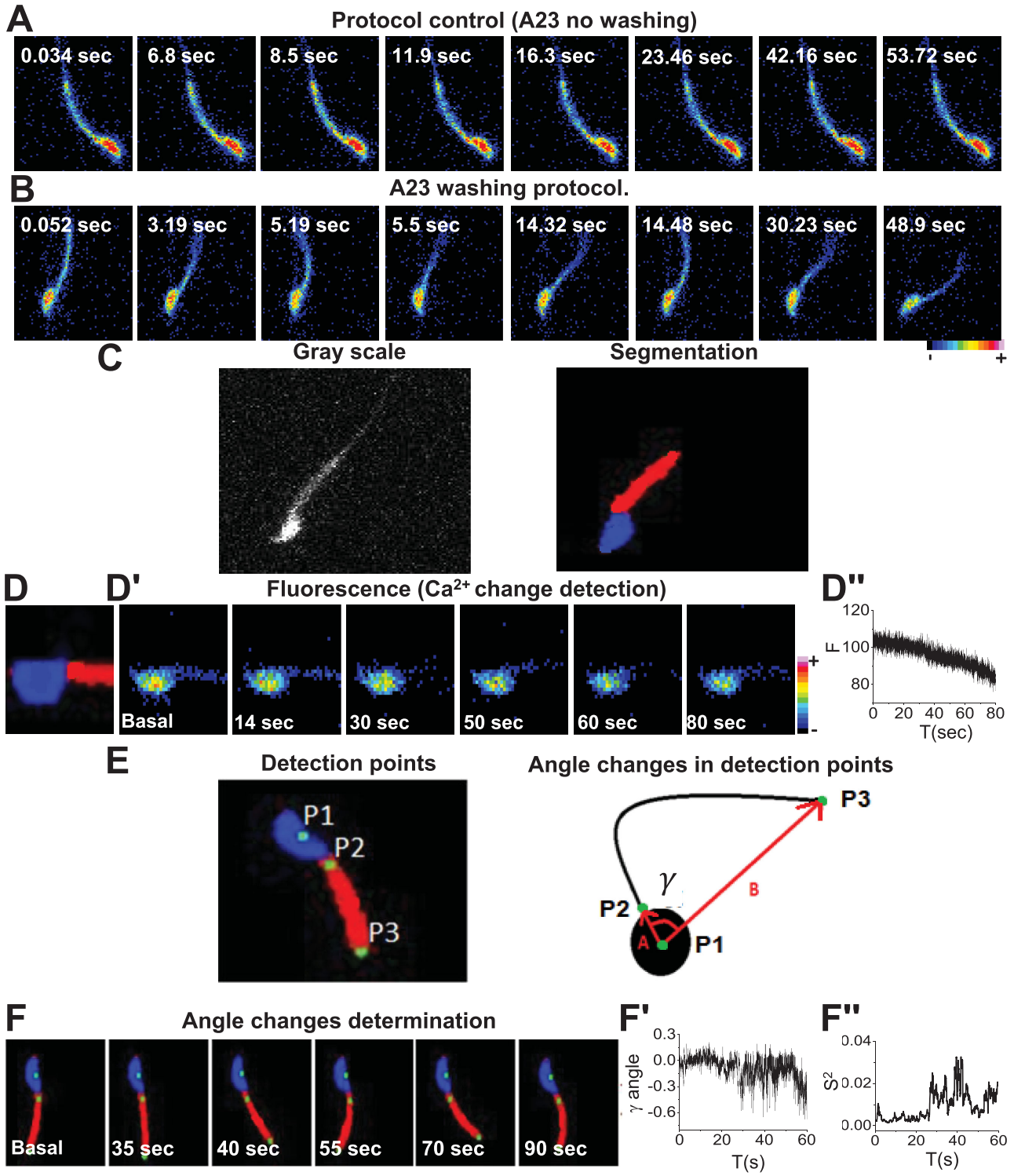

Figure 5. Simultaneous detection of $[Ca^{2+}]_i$ and motility of individual spermatozoa. Fluorescence image sequences at a higher time resolution (at 20–40 FPS) used to implement the simultaneous detection of $[Ca^{2+}]_i$ and flagellar beat of individual spermatozoa. Representative sperm images after: (A) application of 10 μM A23187 (control) and (B) after ionophore washing to recover motility. (C) Gray scale filtered images obtained from the image stack were used to implement the detection method (left panel). From these images a segmented image (right panel) was obtained to monitor changes in head and flagella during automatized parameter detection (see Methods). (D) In the segmented images, the sperm head, shown in blue, was used to detect (D') fluorescence changes. (D") Example of fluorescence changes ($[Ca^{2+}]_i$) detected in the head of one spermatozoon during fast time resolution experiments. In this case, the fluorescence decreased after A23187 removal. (E) Implemented detection points to monitor flagellar midpiece movement (left panel). Diagram illustrating the changes of angle γ evaluated between the points of head and flagellar midpiece used to monitor beating modifications in spermatozoa during the experiments (right panel). (F) γ angle change determination using the detection points to monitor flagellar movement observed in one spermatozoon after A23187 removal. (F') γ angle changes obtained by the automatized program during the experiment in Figure 1F. (F") (S^2). Instantaneous variance of angle changes was used as a useful tool to determine changes in motility. (Please see the online version for the color figure.)

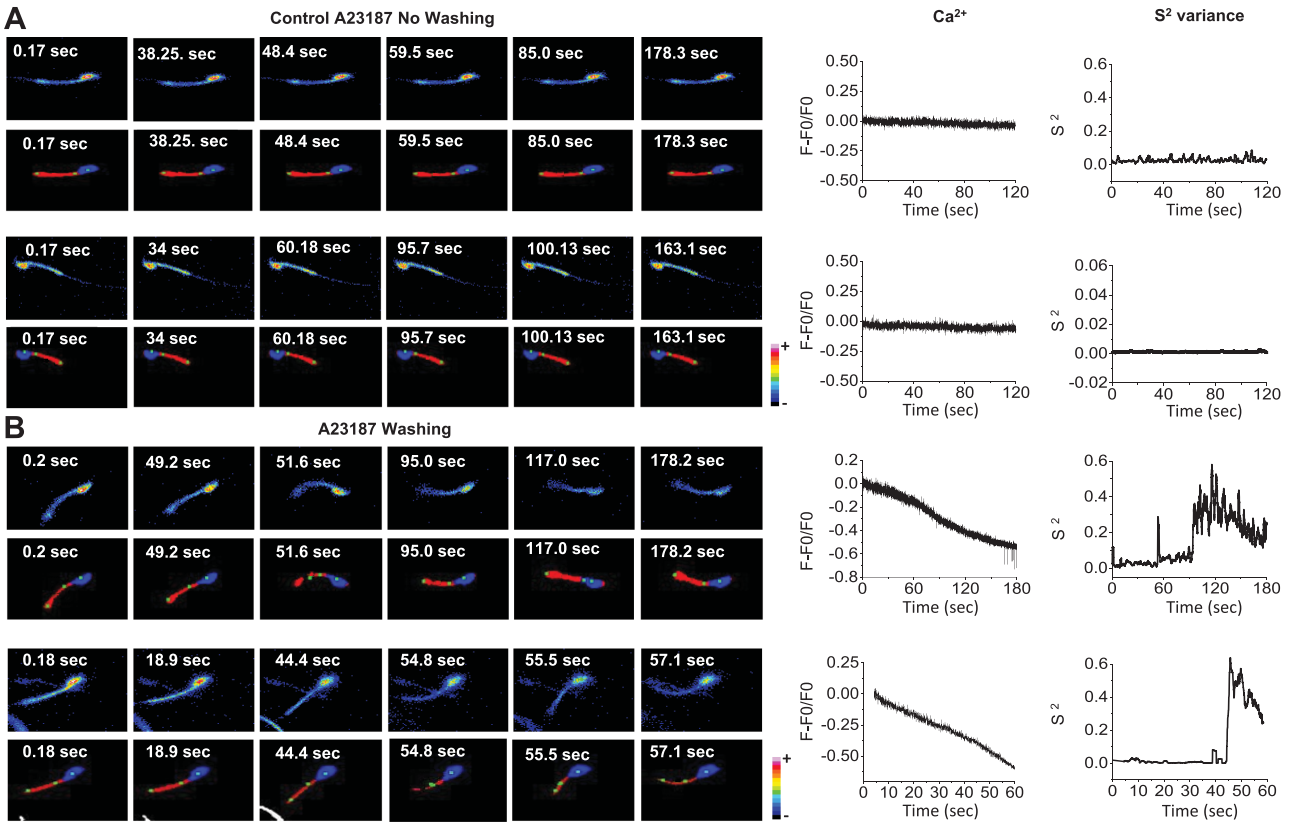

Figure 6. Simultaneous $[Ca^{2+}]_i$ and S^2 changes measured by the automatized detection program in individual spermatozoa. (A) Representative simultaneous time fluorescence images (upper panels) and their corresponding detection points (alternate panels) of spermatozoa after A23187 addition without washing (Control A23187 No Washing). (B) Representative A23187 washing experiments. The traces display changes in $[Ca^{2+}]_i$ (left panels) and S^2 angle of the corresponding sperm (right panels). (Please see the online version for the color figure.)

of these proteins and the axoneme is not known. As $[Ca^{2+}]_i$ is also controlled by transporters and proteins that remove this cation from the cytoplasm (e.g., the plasma membrane Ca^{2+} ATPase PMCA4 and the Na^+/Ca^{2+} exchanger), and by intracellular stores with their corresponding Ca^{2+} ATPase and Ca^{2+} transporters [18], they must also be considered to understand the orchestration of Ca^{2+} in sperm.

The finding mentioned earlier that transiently treating spermatozoa with A23187 overcomes the need for Adcy10 and PKA activation strongly suggests that Ca^{2+} signaling during capacitation is downstream of the cAMP pathway. These data are also consistent with a model in which an initial increase in $[Ca^{2+}]_i$ is required to induce changes in flagellar beating necessary for hyperactivation. However, when the sperm $[Ca^{2+}]_i$ is increased beyond a given threshold, flagellar motility ceases. Once the Ca^{2+} ionophore is washed away, Ca^{2+} removal from the cytoplasm allows the spermatozoon to lower $[Ca^{2+}]_i$ to levels compatible with motility and hyperactivation [6].

In the present work, we tested some of the implications of this model by visualizing flagellar beating and $[Ca^{2+}]_i$ simultaneously in spermatozoa attached to laminin. First, we showed that the effect of A23187 was time and concentration dependent. At all concentrations, addition of A23187 first induced an increase in flagellar beating at 1 min. However, complete loss of motility was observed when ionophore concentrations greater than 1 μM were employed; spermatozoa incubated with 0.5 μM A23187 remained motile. CASAnova analysis of sperm in suspension treated with increasing A23187 concentrations rendered similar results. Initially, all A23187 concentrations induced an increase in the percentage of hyperactive sperm. However, only the 0.5 μM A23187 was able to maintain motility for 1 h and achieve hyperactivation levels comparable with those of capacitated sperm incubated without ionophore. These experiments suggest that while the $[Ca^{2+}]_i$ reached with 0.5 μM A23187 is in the range required for sperm to gain hyperactive motility, higher $[Ca^{2+}]_i$ results in motility loss. As previously shown [5, 19], removing A23187 from the incubation media resulted in complete motility recovery and an elevated percentage of hyperactive sperm.

To further investigate the hypothesis that a threshold $[Ca^{2+}]_i$ exists that mediates whether Ca^{2+} stimulates, or inhibits sperm motility, we simultaneously monitored Fluo-4 fluorescence (correlated with $[Ca^{2+}]_i$) and flagellar beating of laminin-attached spermatozoa. This method was used to analyze sperm treated with 10 μM A23187 for 10 min and washed with media without A23187. Initial experiments indicated that the majority of the A23187-treated sperm recover their motility within 10 min. As these studies were done at a slow frame rate, a faster acquisition rate (10 FPS) was used to detect the exact moment when the sperm flagellum starts to beat, and subsequently correlate this event with $[Ca^{2+}]_i$ changes. Using this higher frame rate, we followed individual sperm for almost 3 min. Every sperm that recovered its motility within this time period showed a decrease in Fluo-4 fluorescence. Given that it is complicated to follow individual sperm in motion, we implemented

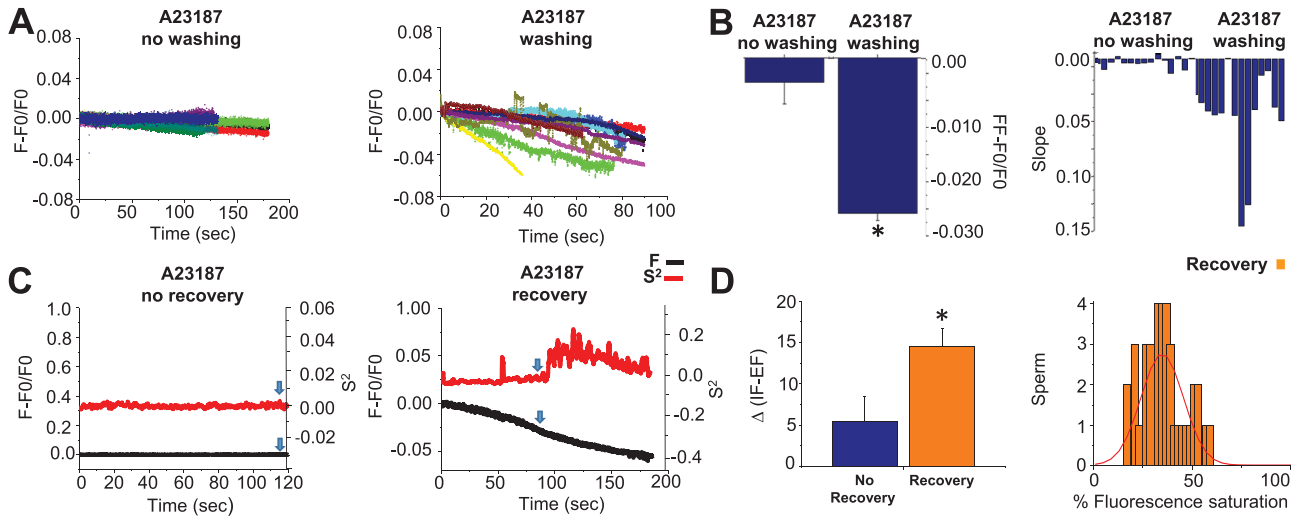

Figure 7. [Ca^{2+}]$_i$ threshold determines motility recovery. (A) Normalized fluorescence changes (F-F0/F0) in time corresponding to A23187 no washing (left panel) or A23187 washing (right panel) protocols. (B) Bars showing average of FF-F0/F0 (final fluorescence-fluorescence after ionophore treatment) of spermatozoa after A23187 no washing and A23187 washing protocols. In the washing case, F0 is the fluorescence just after ionophore removal. Differences are statistically significant ($P = < 0.001$, n = 8 mice). Right panel compares the slopes values obtained from the F-F0/F0 fluorescence traces of sperm exposed to A23187 no washing vs. A23187 washing protocol. (C) Traces corresponding to S^2 changes (red) and normalized (F-F0/F0) fluorescence ([Ca^{2+}]$_i$) (black) for A23187 washed sperm that did not recover or recovered flagellar beating. Blue arrows indicate the moment that fluorescence values were measured for each condition. (D) Left panel shows the Δ value of IF (Initial fluorescence)—EF (End fluorescence) normalized, observed in A23187 treated spermatozoa. EF was considered at the moment S^2 increased above three standard deviations, for the recovery condition, and at the end of the experiment for the nonrecovery condition. The IF-EF differences in these two conditions were statistically significant ($P = 0.02$, n = 10 mice). Right panel illustrates the histogram of the number of sperm displaying defined intervals of fluorescence values at the time when their flagella initiated moving (when S^2 changed as defined above). Fluo-4 fluorescence ranged from 0 to 255, the saturation value inside sperm caused by 10 μM A23187. Fluorescence values were normalized considering 255 as 100%. The histogram is reasonably well fitted by a normal distribution (red). (Please see the online version for the color figure.)

a sensitive semiautomated methodology that segments the sperm head and midpiece, simultaneously measures Fluo-4 fluorescence intensity, and quantifies flagellar midpiece curvature. The algorithm automatically determines three points in the sperm considering the head and midpiece centers of mass, defines two vectors (see Figure 5E and Methods) and measures the angle between them over time. The presence or absence of curvature angle changes correlate to the presence or absence of flagellar beating. We measured the variance of a 50 time point window of this angle as a function of time (S^2) to detect when sperm start moving. Once movement was detected, the level of Fluo-4 fluorescence intensity relative to the initial fluorescence value, corresponding to the moment or flagellar beating transition, was determined.

Our observations indicate that there is a correlation between a defined range of [Ca^{2+}]$_i$ and the initiation of flagellar beating, as detected by a sudden S^2 increase. As expected, the [Ca^{2+}]$_i$ level of A23187 treated-then-washed spermatozoa was significantly lower than concentrations determined in nonwashed spermatozoa. In addition, washed cells showed a defined rate of [Ca^{2+}]$_i$ decrease that was not observed in nonwashed cells. On the other hand, some of the washed cells did not recover motility in the recorded 3-min time window. When comparing A23187 washed sperm that did not recover with those that recovered, cells with higher S^2 values and flagellar movement display a significantly larger and faster rate of [Ca^{2+}]$_i$ decrease. Finally, the distribution of fluorescence values ([Ca^{2+}]$_i$ levels), within the full fluorescence range, displayed by sperm at the time flagellar beating initiates is consistent with the existence of a [Ca^{2+}]$_i$ threshold. Overall, our findings suggest that after losing motility due to a large [Ca^{2+}]$_i$ increase caused by A23187, ionophore removal leads to a [Ca^{2+}]$_i$ decrease, which upon reaching a threshold, permits mouse sperm flagella to regain movement.

Earlier work had established in detergent-treated mammalian sperm that there is a Ca^{2+} dependence on flagellar curvature [20, 21]. In these experiments increasing Ca^{2+} levels, within a physiologically relevant range, resulted in more asymmetric flagellar beating. In addition, high Ca^{2+} concentrations inhibited flagellar movement [22, 23]. Though not fully established, evidence is consistent with the hypothesis that Ca^{2+} differentially affects distinct dynein arms of the axoneme to influence beat cycle parameters [3, 24, 25]. In nonmammalian sperm axonemes, Ca^{2+}-sensitive elements have been found in the outer arms [26, 27, 28] in the drc/nexin [29], and on the spoke shafts [30]. In addition, Ca^{2+}-binding proteins such as Calmodulin and Centrin have been reported associated to the mammalian sperm axoneme [31]. Therefore, our observations are consistent with [Ca^{2+}]$_i$ finely orchestrating when and how the sperm flagella beats.

Ca^{2+} appears to disproportionately influence dynein motors situated on one side of the ring of dynein doublets [3, 25, 32]. It is suspected that high [Ca^{2+}]$_i$ levels may lock certain dyneins into a sustained activation state which impedes switching with the period of the beat cycle [32, 33, 34], due to the production of force and bending torque acting to bend the flagellum in one direction. This would explain why high [Ca^{2+}]$_i$ arrests many types of cilia and flagella [35].

In the present work, we have found, using the ionophore A23187 as a tool to control [Ca^{2+}]$_i$, that it is likely that there are at least two thresholds: one above which the flagellum immobilizes and below which flagellar beating starts and eventually becomes asymmetric,

and a lower one where beating is more symmetrical and constant. It is known that detergent demembranated flagella from several mammalian sperm beat in an activated manner in the presence of ATP with as low as 30 nM of Ca^{2+}. Raising Ca^{2+} to around 100 nM initiates hyperactivation which is fully achieved at hundreds of nM [25, 36]. These values are not far from $[Ca^{2+}]_i$ determined in live mammalian sperm [37]. Interestingly, fast $[Ca^{2+}]_i$ oscillations that correlated to the beating flagellar frequency have been reported in hamster spermatozoa swimming in a restricted volume [37], and very recently in human spermatozoa flagella beating in three dimensions. These detected fast $[Ca^{2+}]_i$ oscillations, which are independent of Ca^{2+} uptake through ionic channels and are correlated with flagellar beating frequency, could reflect changes in the association of this ion with Ca^{2+}-binding proteins that regulate axonemal beating [38].

Surprisingly, once utilized to in vitro fertilize oocytes, sperm treated with ionophore increased the percentage of two-cell embryos arriving to blastocyst stages. Considering that A23187 has already been used in the clinical setting to activate metaphase II-arrested oocytes, applying a pulse of A23187 has potential to be used to treat sperm from infertile patients. This potential clinical application highlights the relevance of understanding the role of $[Ca^{2+}]_i$ thresholds at the basic level documented in the present work. Our novel strategy to follow simultaneously $[Ca^{2+}]_i$ and motility in sperm recovering from A23187 treatment could potentially allow studies of the dynamics of $[Ca^{2+}]_i$ signals that regulate sperm hyperactivation. The next step will be to establish quantitatively the concentration value of those thresholds involved in the regulation of different flagellar beating modes. Precise measurement of $[Ca^{2+}]_i$ values can be accomplished using either ratiometric dyes or two different dyes recorded simultaneously at fast rates (thousands/s). These experiments are challenging and required the use of new and improved acquisition techniques. However, advancement in detection systems, the possibility of using transgenically encoded dyes [39], and the continuous development of faster recording cameras presuppose that precise and quantitative $[Ca^{2+}]_i$ measurements in sperm will be accomplished.

Supplementary data

Supplementary data are available at *BIOLRE* online.

Supplemental Figure S1. CASA motility parameters. Motility parameters measured by CASA obtained at different experimental conditions. (A) Control sperm (no A23187 added) during capacitation. Sperm treated with the following A23187 concentrations: (B) 0.5 μM, (C) 1 μM, (D) 5 μM, and (E) 10 μM of A23187. (F) Sperm treated with 20 μM of A23187 for 10 min and then washed by centrifugation. Measurements were done at 5, 15, 30, and 45 min except for A23187 wash, where one extra time point at 60 min was taken. Bars represent average ± SEM. The percentage of the indicated parameter was obtained using CASAnova software (n = 3); S = slow, W = weak, I = intermediate, P = Progressive, TM = Total motility.

Supplemental Figure S2. Area change detection. (A) Pixel map from a segmented sperm. These maps were used to detect focus variations during the automatized parameter recordings. (B) Changes in area pixels detected while one sperm defocuses during the recording. (C) Area in pixels plotted during automatized detection.

Supplemental Movie 1. Fluorescence recording showing that A23187 addition promotes a rapid and sustained $[Ca^{2+}]_i$ increase in all sperm in the field. The movie corresponds to 10 min of recording and was acquired at 0.2 FPS.

Supplemental Movie 2. Fluorescence imaging showing a higher magnification of the field in Movie 1.The recording shows two cells that increase flagellar beating after A23187 application before becoming completely immobilized. The movie corresponds to 10 min of recording acquired at 0.2 FPS.

Supplemental Movie 3. Fluorescence video illustrating a field of sperm exposed to 10 μM A23187. The movie corresponds to 2 min of recording and was acquired at 8 FPS.

Supplemental Movie 4. Fluorescence time images showing that after a 10 μM A23187 addition the $[Ca^{2+}]_i$ levels and sperm immobilization are maintained during 30 min of recording. The movie was acquired at 0.2 FPS.

Supplemental Movie 5. Fluorescence imaging shows that A23187 washing decrease $[Ca^{2+}]_i$ and restores flagellar beating sperm. The movie corresponds to 45 min of recording acquired at 0.2 FPS.

Acknowledgments

We are grateful for the excellent technical assistance of José Luis de la Vega Beltrán from IBT UNAM and Nicolas Jiménez from IFC UNAM. We also appreciate the fine computational support of Ana Maria Escalante and Francisco Pérez from the Computing Unit of IFC UNAM and Omar Arriaga from the IBT UNAM. The authors are also indebted to Diana Millán-Aldaco and Ruth Rincón-Heredia for technical assistance and MVZ Claudia V. Rivera-Cerecedo for animal breeding and management. We thank Dr Chris Wood for critically editing our manuscript.

References

1. Gervasi MG, Visconti PE. Chang's meaning of capacitation: A molecular perspective. *Mol Reprod Dev* 2016; **83**:860–874.
2. Chang H, Suarez SS. Rethinking the relationship between hyperactivation and chemotaxis in mammalian sperm. *Biol Reprod* 2010; **83**:507–513.
3. Lindemann CB, Lesich KA. Functional anatomy of the mammalian sperm flagellum. *Cytoskeleton* 2016; **73**:652–669.
4. Tateno H, Mikamo K. A chromosomal method to distinguish between X- and Y-bearing spermatozoa of the bull in zona-free hamster ova. *Reproduction* 1987; **81**:119–125.
5. Tateno H, Krapf D, Hino T, Sánchez-Cárdenas C, Darszon A, Yanagimachi R, Visconti PE. Ca2+ ionophore A23187 can make mouse spermatozoa capable of fertilizing in vitro without activation of cAMP-dependent phosphorylation pathways. *Proc Natl Acad Sci USA* 2013; **110**:18543–18548.
6. Navarrete FA, Alvau A, Lee HC, Levin LR, Buck J, Leon PM, Santi CM, Krapf D, Mager J, Fissore RA, Salicioni AM, Darszon A, et al. Transient exposure to calcium ionophore enables in vitro fertilization in sterile mouse models. *Sci Rep* 2016; **15**:33589.
7. Espinal-Enríquez J, Priego-Espinosa DA, Darszon A, Beltrán C, Martínez-Mekler G. Network model predicts that CatSper is the main Ca2+ channel in the regulation of sea urchin sperm motility. *Sci Rep* 2017; **7**:4236.
8. Olson SD, Suarez SS, Fauci LJ. Coupling biochemistry and hydrodynamics captures hyperactivated sperm motility in a simple flagellar model. *J Theor Biol* 2011; **283**:203–216.
9. Goodson SG, Zhang Z, Tsuruta JK, Wang W, O'Brien DA. Classification of mouse sperm motility patterns using an automated multiclass support vector machines model. *Biol Reprod* 2011; **84**:1207–1215.
10. Qi H, Moran MM, Navarro B, Chong JA, Krapivinsky L, Kirichok Y, Ramsey IS, Quill TA, Clapham DE. All four CatSper ion channel proteins are required for male fertility and sperm cell hyperactivated motility. *Proc Natl Acad Sci USA* 2007; **104**:1219–1223.
11. Kirichok Y, Navarro B, Clapham DE. Whole-cell patch-clamp measurements of spermatozoa reveal an alkaline-activated Ca2+ channel. *Nature* 2006; **439**:737–740.

12. Ren D, Ren D, Navarro B, Perez G, Jackson AC, Hsu S, Shi Q, Tilly JL, Clapham DE. A sperm ion channel required for sperm motility and male fertility. *Nature* 2001; **413**:603–609.
13. Liu J, Xia J, Cho KH, Clapham DE, Ren D. CatSperβ, a novel transmembrane protein in the CatSper channel complex. *J Biol Chem* 2007; **282**:18945–18952.
14. Wang H, Liu J, Cho KH, Ren D. A novel, single, transmembrane protein CATSPERγ is associated with CATSPER1 channel protein. *Biol Reprod* 2009; **81**:539–544.
15. Chung JJ, Miki K, Kim D, Shim SH, Shi HF, Hwang JY, Cai X, Iseri Y, Zhuang X, Clapham DE. CatSperζ regulates the structural continuity of sperm Ca2+ signaling domains and is required for normal fertility. *Elife* 2017; **23**:e23082.
16. Chung JJ, Navarro B, Krapivinsky G, Krapivinsky L, Clapham DE. A novel gene required for male fertility and functional CATSPER channel formation in spermatozoa. *Nat Commun* 2011; **11**:153.
17. Chung JJ, Shim SH, Everley RA, Gygi SP, Zhuang X, Clapham DE. Structurally distinct Ca (2+) signaling domains of sperm flagella orchestrate tyrosine phosphorylation and motility. *Cell* 2014; **157**:808–822.
18. Raffaello A, Mammucari C, Gherardi G, Rizzuto R. Calcium at the center of cell signaling: interplay between endoplasmic reticulum, mitochondria, and lysosomes. *Trends Biochem Sci* 2016; **41**:1035–1049.
19. Suarez SS, Vincenti L, Ceglia MW. Hyperactivated motility induced in mouse sperm by calcium ionophore A23187 is reversible. *J Exp Zool* 1987; **244**:331–336.
20. Lindemann CB, Goltz JS. Calcium regulation of flagellar curvature and swimming pattern in triton X-100-extracted rat sperm. *Cell Motil Cytoskeleton* 1988; **10**:420–431.
21. Marquez B, Ignotz G, Suarez SS. Contributions of extracellular and intracellular Ca2+ to regulation of sperm motility: release of intracellular stores can hyperactivate CatSper1 and CatSper2 null sperm. *Dev Biol* 2007; **303**:214–221.
22. Tash JS, Means AR. Ca2+ regulation of sperm axonemal motility. *Methods Enzymol* 1987; **139**:808–823.
23. Tash JS, Means AR. cAMP-dependent regulatory processes in the acquisition and control of sperm flagellar movement. *Prog Clin Biol Res* 1988; **267**:335–355.
24. Lesich KA, Kelsch CB, Ponichter KL, Dionne BJ, Dang L, Lindemann CB. The calcium response of mouse sperm flagella: role of calcium ions in the regulation of dynein activity. *Biol Reprod* 2012; **86**:105.
25. Ishijima S. Ca2+ and cAMP regulations of microtubule sliding in hyperactivated motility of bull spermatozoa. *Proc Jpn Acad Ser B Phys Biol Sci* 2015; **91**:99–108.
26. King SM, Patel-King RS. Identification of a Ca (2+)–binding light chain within Chlamydomonas outer arm dynein. *J Cell Sci* 1995; **108**:3757–3764.
27. Sakato M, Sakakibara H, King SM. Chlamydomonas outer arm dynein alters conformation in response to Ca2+. *Mol Biol Cell* 2007; **18**:3620–3634.
28. Mizuno K, Shiba K, Okai M, Takahashi Y, Shitaka Y, Oiwa K, Tanokura M, Inaba K. Calaxin drives sperm chemotaxis by Ca2+-mediated direct modulation of a dynein motor. *Proc Natl Acad Sci USA* 2012; **109**:20497–20502.
29. LeDizet M, Piperno G. The light chain p28 associates with a subset of inner dynein arm heavy chains in Chlamydomonas axonemes. *Mol Biol Cell* 1995; **6**:697–711.
30. Yang P, Diener DR, Yang C, Kohno T, Pazour GJ, Dienes JM, Agrin NS, King SM, Sale WS, Kamiya R, Rosenbaum JL, Witman GB. Radial spoke proteins of Chlamydomonas flagella. *J Cell Sci* 2006; **119**:1165–1174.
31. Viswanadha R, Sale WS, Porter ME. Ciliary motility: regulation of axonemal dynein motors. *Cold Spring Harb Perspect Biol* 2017; **9**: a018325.
32. Lesich KA, dePinho TG, Dionne BJ, Lindemann CB. The effects of Ca2+ and ADP on dynein switching during the beat cycle of reactivated bull sperm models. *Cytoskeleton* 2014; **71**:611–627.
33. Brokaw CJ. Calcium-induced asymmetrical beating of triton-demembranated sea urchin sperm flagella. *J Cell Biol* 1979; **82**:401–411.
34. Eshel D, Brokaw CJ. New evidence for a "biased baseline" mechanism for calcium-regulated asymmetry of flagellar bending. *Cell Motil Cytoskeleton* 1987; **7**:160–168.
35. Lindemann CB, Lesich KA. The geometric clutch at 20: stripping gears or gaining traction? *Reproduction* 2015; **150**:R45–R53.
36. Ho HC, Suarez SS. Hyperactivation of mammalian spermatozoa: function and regulation. *Reproduction* 2001; **122**:519–526.
37. Suarez SS, Varosi SM, Dai X. Intracellular calcium increases with hyperactivation in intact, moving hamster sperm and oscillates with the flagellar beat cycle. *Proc Natl Acad Sci USA* 1993; **90**:4660–4664.
38. Corkidi G, Montoya F, Hernández-Herrera P, Ríos-Herrera WA, Müller MF, Treviño CL, Darszon A, Are there intracellular Ca2+ oscillations correlated with flagellar beating in human sperm? A three vs. two-dimensional analysis. *Mol Hum Reprod* 2017; **9**:583–593.
39. Niwa F, Sakuragi S, Kobayashi A, Takagi S, Oda Y, Bannai H, Mikoshiba K. Dissection of local Ca(2+) signals inside cytosol by ER-targeted Ca(2+) indicator. *Biochem Biophys Res Commun* 2016;**479**:67–73.